

1 **Reply to Comment on Franz et al. (2023): A reinterpretation of the 1.5 billion year old Volyn**
2 **'biota' of Ukraine, and discussion of the evolution of the eukaryotes, by Head et al. (2023)**

3
4 **Gerhard Franz¹, Vladimir Khomenko^{1,2}, Peter Lyckberg³, Vsevolod Chornousenko⁴, Ulrich**
5 **Struck⁵**

6 ¹Institut für Angewandte Geowissenschaften, Technische Universität Berlin, D-10587 Berlin,
7 Germany

8 ²M.P. Semenenko Institute of Geochemistry, Mineralogy and Ore Formation, The National
9 Academy of Sciences of Ukraine, 34, Palladina av., Kyiv, 03142, Ukraine

10 ³Luxembourg National Museum of Natural History, 25 Rue Münster, 2160 Luxembourg,
11 Luxembourg

12 ⁴Volyn Quartz Samotsvety Company, Khoroshiv (Volodarsk-Volynski), Ukraine*

13 ⁵Museum für Naturkunde Berlin, Invalidenstraße 43, D-10115 Berlin, Germany

14 *now at: Kondratyuka str. 9, ap. 25, Zhytomyr, 10009 Ukraine

15
16 Correspondence: Gerhard Franz (gerhard.franz@tu-berlin.de; gefra548@gmail.com)

17
18 **Abstract.** Head et al. (2023) emphasize the importance of the Volyn biota for the evolution,
19 especially in the so-called 'boring billion', in a detailed outline about the biological and
20 geological context. However, they question that the Volyn biota represent Precambrian fossils
21 and instead argue that they contain young contaminants of 'museum dust'. In addition, they
22 question their biotic origin. We present here a detailed discussion of their points of concern
23 based on presented data, including some additional information. Their points of concern
24 were:

- 25 - One object, shown by Franz et al. (2023) is similar to a pollen grain, another object is
26 similar to trichomes; we show indications for fossilization and summarize our
27 arguments against 'museum dust'.
- 28 - They question the fossil character of the biota and argue for a biomineralization; we
29 show that the biomineralization in trichomes is distinct from the mineralization of the
30 biota.
- 31 - They missed information about the internal structure; we repeat the presented
32 information about the internal structure in more detail, which is also indicative of fossil
33 material and inconsistent with trichomes.
- 34 - They argue that we did not compare via infrared spectroscopy the biota with recent
35 fungi; since the biota experienced temperatures near 300°C, we think that a
36 comparison with thermally degraded chitosan is more appropriate.
- 37 - They question the use of strongly negative $\delta^{13}\text{C}$ as an argument for biotic origin, but
38 we show that in combination with positive $\delta^{15}\text{N}$ values and the geological situation, a
39 biotic origin is more likely than abiotic synthesis.

40 In addition, Popov (2023) questioned the age of the Volyn biota, which we postulated as
41 between approximately 1.5 and 1.7 Ga. He argues that the fossils could be Phanerozoic. We
42 will also outline our arguments for the minimum age of 1.5 Ga.

43
44 **1 Introduction**

hat formatiert

hat formatiert: Schriftart: (Standard) +Textkörper (Calibri)

hat formatiert: , Nicht Hochgestellt/ Tiefgestellt

hat gelöscht: |

Feldfunktion geändert

Feldfunktion geändert

hat gelöscht: are

hat gelöscht: postulate that they are of a-

48 We thank Head et al. (2023) for stimulating the discussion about the Volyn biota. They
49 question that these are fossils, instead argue that at least some of them are young
50 contaminants by plant hairs and pollen. This could have occurred during storage as what they
51 called 'museum dust' or during sampling. Furthermore, they question the biogenicity and
52 argue for an abiotic origin. We appreciate their comment, because this question of
53 contamination was not raised before, neither in our papers from 2017, 2022, and 2023, nor in
54 any of the previous publications about kerite from Volyn.

1.1 Review of kerite formation

The words 'kerite' and 'kerogen' are derived from the Greek word $\kappa\eta\rho\acute{o}\varsigma$ (*kērós*) meaning "wax". Kerogen is the insoluble residue of organic matter in sedimentary rocks that is left after its treatment by common organic solvents (Durand 1980); the soluble fraction is called bitumen. With increasing temperature, solid oil bitumens range from asphaltite over kerite to anthraxolite; kerite (high and low) has a density of 1.05-1.3; an atomic C/(C+H+N+O) of 0.39-0.62, H/C (at) of 0.59-1.44, a composition (in wt%) of 69-91 C; 4.5-9 H, 0.5-2 N, 1-12 O (Moroz et al. 1998). Moroz et al. (1998) and Ciarniello et al. (2019) also considered kerite as an analog for extraterrestrial organic matter.

Kerite from the Volyn occurrence was first described as an abiogenic material (Ginzburg et al., 1987; Luk'yanova et al., 1992) and as a prime example of protein synthesis by inorganic processes (Yushkin 1996). Its composition is given as (wt%) C 76.51; H 5.02; O+N 17.46; S 0.42; Cl 0.24; Fe 0.06; Cu 0.15 with a chemical formula $C_{491}H_{386}O_{87}S(N)$. Among many minor impurities Yushkin (1996) lists Si, Al, Na, K, and Mg, and he mentions very light isotopic $\delta^{13}C$ of -40 ‰. However, kerite from Volyn was later reinterpreted as fossilized cyanobacteria (Gorlenko et al., 2000; Zhmur, 2003), transported in a geyser system from ponds at the surface into the depth, where it is found now in cavities of pegmatitic rocks.

1.2 Discussion points

The main points of discussion are the i) possible contamination during or after sampling; ii) the type of the kerite organic matter including its chemical composition and its structure; iii) the morphology of the different objects, as observed under the scanning electron microscope (SEM) and comparison what Head et al. (2023) described as contamination; iv) the available age constraints of the fossils and further possibilities for dating; and, finally, v) a summary with the open questions.

2 Occurrence of kerite and sampling

The following information is based on logbooks from the mine (VC, mine geologist in the area since 1990) who also collected the material for our study together with PL. The samples of kerite occur in situ underground in several, but not all shafts of the Volyn pegmatite district. Within the large, miarolitic cavities ('chambers' in the original literature) kerite is also found in the mineral matrix (feldspar, mica, clay minerals) on the floor of the pegmatite and is also hanging from the walls or the ceiling. However, kerite in visible amounts is not preserved in most chambers. It was either destroyed during cleaning and gemstone extraction, or it was already collected. In those chambers which were explored by drilling, it was completely destroyed by drilling fluids mixed with clay that covered the whole ground of the chambers. Well-preserved large amounts of kerite were found only in new pockets opened by miners underground without drilling. In January 2013 kerite was found (PL) in a 5 mm wide zone around topaz crystals on the wall of a 15 m tall chamber in shaft 3. Kerite was observed growing at the base of dark lilac to black fluorite crystals, in larger fiber masses around large

hat nach unten verschoben [2]: who either described kerite as an abiogenic material (Ginzburg et al., 1987; Luk'yanova et al., 1992; Yushkin 1996, 1998) or as fossilized cyanobacteria (Gorlenko et al., 2000; Zhmur, 2003).

hat formatiert: Schriftart: (Standard) +Textkörper (Calibri)

hat formatiert: Schriftart: Fett, Schriftfarbe: Schwarz

Formatiert: Listenabsatz, Mit Gliederung + Ebene: 2 + Nummerierungsformatvorlage: 1, 2, 3, ... + Beginnen bei: 1 + Ausrichtung: Links + Ausgerichtet an: 0 cm + Einzug bei: 0.63 cm

hat formatiert: Schriftart: (Standard) +Textkörper (Calibri)

hat formatiert: Schriftart: (Standard) +Textkörper (Calibri)

hat formatiert: Schriftart: (Standard) +Textkörper (Calibri)

hat formatiert: Schriftart: (Standard) +Textkörper (Calibri)

hat formatiert: Schriftart: (Standard) +Textkörper (Calibri)

hat formatiert: Schriftart: (Standard) +Textkörper (Calibri)

hat formatiert: Schriftfarbe: Schwarz

hat formatiert: Schriftart: (Standard) +Textkörper (Calibri)

hat formatiert: Schriftart: (Standard) +Textkörper (Calibri), Englisch (USA)

hat formatiert: Schriftart: (Standard) +Textkörper (Calibri)

Formatiert: Einzug: Erste Zeile: 1 cm, Abstand Vor: 0 Pt., Nach: 0 Pt.

hat formatiert: Schriftfarbe: Schwarz

hat formatiert: Schriftfarbe: Schwarz

hat formatiert: Schriftfarbe: Schwarz

hat formatiert: Schriftart: Symbol

hat formatiert: Hochgestellt

hat formatiert: Schriftfarbe: Schwarz

hat formatiert: Schriftfarbe: Schwarz

hat formatiert: Schriftart: (Standard) +Textkörper (Calibri)

hat formatiert: Schriftart: (Standard) +Textkörper (Calibri)

hat formatiert: Schriftart: (Standard) +Textkörper (Calibri), Fett, Englisch (USA)

hat verschoben (Einfügung) [2]

hat gelöscht: who either described kerite as an abiogenic material (Ginzburg et al., 1987; Luk'yanova et al., 1992; Yushkin 1996, 1998) or as fossilized cyanobacteria (Gorlenko et al., 2000; Zhmur, 2003)....

102 topaz crystals, as larger fiber masses in clay along the lower walls and as large masses on well
103 crystallized feldspars, mica, quartz and topaz high on the walls in two chambers.

104 Early descriptions in the drilling logbooks mention in some cases that chambers were full
105 of kerite, up to 25 kg of kerite(!) in the rather small pegmatite body from shaft 3, which has
106 accesses to several pegmatite bodies (consistent with reports in the literature, e. g. Ginzburg
107 et al., 1987). Material from this shaft was distributed to museums in the former Soviet Union.
108 The chambers are now in a depth of up to 96 m, some were mined in open pits, but the
109 crystallization depth of the pegmatites was at a depth corresponding to 2-3 kbar. Thus,
110 significant uplift had occurred since intrusion at 1.76 Ga, but there is no indication from the
111 geological literature of the area that the chambers were directly on or beneath the surface
112 and buried again later. Therefore, contamination within the chambers by plant roots going
113 down to 96 m is less likely. In any case, we have no doubt that kerite is part of the deep
114 biosphere. Most trichomes (plant hairs) are known from plants on the surface, not from deep
115 biosphere.

116 Samples kerite 1 to kerite 7 were sampled underground by PL and VC, put into firmly
117 closed plastic sample bags (double ones with label in outer one), transported first to
118 Luxemburg and then sent to Berlin. There was no need to separate kerite from the rocks and
119 from the soil, the material could be picked up. Sample bags were opened only in the electron
120 microscopy laboratory of TU Berlin, which is a special building for electron microscopy with
121 the appropriate arrangements to prevent contamination by dust. All rooms are equipped with
122 airlocks for climatization and in addition water-cooled ceilings minimizes airstream and dust
123 movement in the rooms. Samples were prepared in an exhaust hood. Of course, we cannot
124 completely rule out that some objects are contaminants, but the overwhelming majority of
125 objects on the aluminum sample holders for SEM are original as recovered from underground.
126 The only kerite sample, which could have been contaminated in a museum is our sample
127 'kerite 0'.

128 The beryl crystal sample V2008 was collected from the mine tailings in 2008 by GF, stored
129 at TU Berlin in a common wooden rock cabinet. For this sample, contamination on the mine
130 tailings or later is possible.

131 The breccia with the beryl pseudomorph was also collected from the mine tailings in 2008
132 by GF, stored at TU Berlin in a common wooden rock cabinet, and consolidated with epoxy for
133 preparation of thin sections and polished blocks for the Ar-Ar-determination of muscovite.

134

135 **3 Composition and structure of kerite**

136 **3.1 Organic matter in the beryl pseudomorph**

137 We start the discussion with the OM in the pseudomorph. For this, a later contamination can
138 safely be excluded, as it was discovered in thin sections. It is closely surrounded and
139 intergrown with macroscopically black, in thin section brown, C-H-bearing opal (Franz et al.
140 2017; see their fig. 6). The chemical composition of the OM is characterized by a high amount
141 of Zr, Y, Sc, and REE. These high fieldstrength elements (HFSE) are positively correlated with
142 O, and increasing O contents are correlated with decreasing C contents. The N content is
143 between 2 and 4 at%, much lower than the original kerite (see their fig. 7), which has near 8-
144 9 at% (Ginzburg et al., 1987; Yushkin, 1996). Mobilization of HFSE is possible with a F-rich fluid
145 (Loges et al. 2023), and a high F-content in the system is likely because the pegmatites
146 themselves belong to the Nb-Y-F-type and contain a high amount of topaz. In addition, the
147 muscovite in the breccia is F-rich, and fluorite is a common mineral associated with kerite (see
148 below). For further details such as transmission electron microscopy (TEM) of the border zone
149 of OM to opal and about opal itself, the reader is referred to our original publication.

Kommentiert [01]: Already defined above

hat gelöscht: scanning electron microscopy (

hat gelöscht:)

152 We postulated that the low N-content was caused by decay of kerite, producing NH₄,
153 which was responsible for K-NH₄ exchange reactions in K-feldspar and in muscovite, forming
154 buddingtonite and tobelite. There is no doubt that before the formation of the breccia and
155 the pseudomorph, OM was present in the system. Buddingtonite is not a rare mineral in the
156 Volyn pegmatite field (Proshko, 1987) and the high activity ratio for NH₄⁺/K⁺ required to
157 transform K-feldspar into buddingtonite (Mäder et al., 1996) indicates a large amount of
158 decayed OM. This is not consistent with Head et al.'s concern that the OM in the pegmatite
159 field is late-stage contamination. Also, the chemical composition of the OM is completely
160 incompatible with anything like museum dust or plant hairs.

161 162 **3.2 Fossil or non-fossilized OM**

163 Head et al. (2023) question the fossil character of kerite. Here we want to summarize the
164 presented information about the metamorphic, mature character of kerite.

165 After the occurrence of OM in the pegmatitic environment, the temperatures had
166 reached again approximately 300 °C (Franz et al. 2017). This estimate is based on the phase
167 equilibria with bertrandite and muscovite in the pseudomorph. Furthermore, within beryl we
168 observed fluid inclusions with C-H, which occur on cracks sealed by secondary beryl (Vozniak
169 et al., 2012). This implies that temperatures were above the lower thermal stability of beryl,
170 which is at low pressure near 300 °C (Barton and Young, 2002). These temperatures are
171 consistent with our observation on decomposition of chitin to chitosan described in detail in
172 Franz et al. (2023a), see below the discussion about FTIR data.

173 All kerite samples were investigated by open-system pyrolysis. They do not differ
174 significantly, and all spectra show characteristics of mature to very mature OM (figure 13 in
175 Franz et al. 2022, and in supplement). This excludes young contamination by plant hairs.
176 Similarly, the light microscopic investigations in cross sections with white and UV light show
177 clear indications by different reflectivity and fluorescence, not consistent with young OM. We
178 described brittle behavior of kerite, also not compatible with young unmetamorphosed OM.
179 Brittle behavior was also noted by Yushkin (1996). Luk'ynaova et al. (1982) described X-ray
180 diffraction investigations with a diffuse peak at 8° Theta indicating OM with some graphite-
181 like sheets.

182 Head et al. (2023) refer to mineralized trichomes (Mustafa et al. 2017, 2018; Ensikat et al.
183 2017) and take this as an argument against fossilization. These plant hairs are biomineralized
184 with Ca-carbonate, Ca-phosphate and silica, especially at the tip of the trichomes. This
185 biomineralization is quite different from what we interpreted as fossilized and mineralized
186 rims of the Volyn kerite. We wrote that the most conspicuous feature is the common
187 occurrence of Si-Al-O, interpreted as Al-silicates. In the quoted investigations Al was never
188 observed. Furthermore, Ca-phosphate was observed in kerite only at some places at nano-
189 sized crystals (see e.g. figure 11 in Franz et al. 2022), at variance with a continuous
190 biomineralization on the tips. Kerite is completely surrounded by a mineralized rim, whereas
191 trichomes are only mineralized at their tips. All different kerite morphologies are mineralized
192 in the same way.

193 Concerning the analytical procedure applied by us, there is a misunderstanding in Head
194 et al.'s (2023) comment. On line 146 to 149 they wrote: "Had Franz et al. (2023) used EDX in
195 addition to applying EDAX EDS to selected cross sections, they would have been easily able to
196 determine the elemental distribution for all specimens they imaged using SEM which could
197 have assisted in discriminating extant contaminations from fossil material." For our element
198 mapping we used wave length dispersive (WDS) analysis with the electron microprobe (EMP),
199 which is much more sensitive than energy dispersive systems (EDS) such as EDAX. We have

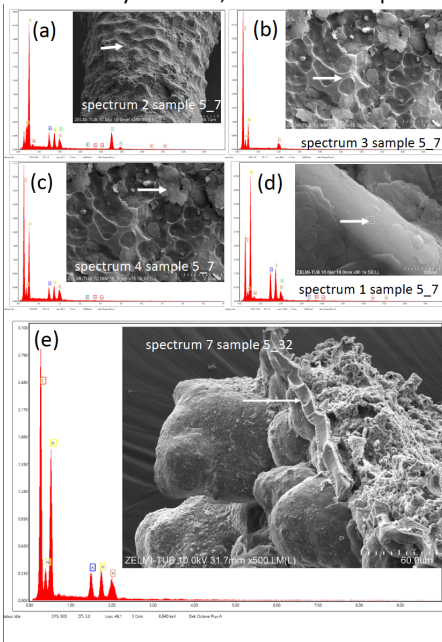
hat gelöscht: s

hat gelöscht:

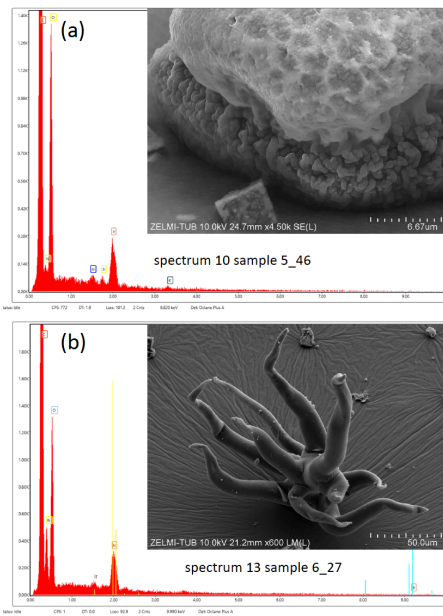
202 shown several element distribution maps of different morphologies in Franz et al. (2022), and
203 since all show generally identical features with an Al-Si-Ca rim structure and an internal
204 structure with characteristic N-O-S distribution, we can safely exclude biomineralization, but
205 instead mineralization due to a fossilization process.

206
207 **3.3 EDS (with SEM)**

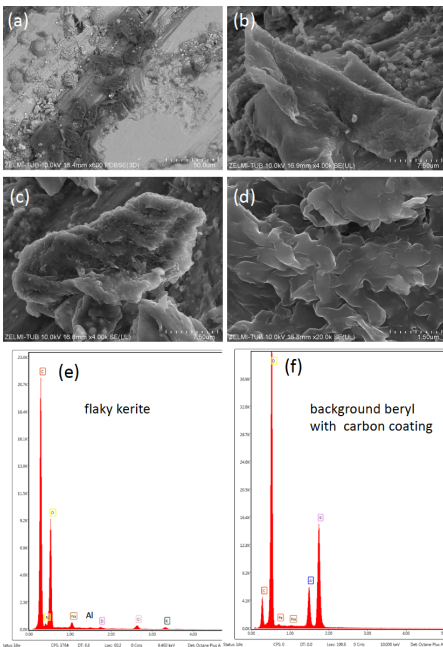
208 All spectra of kerite objects show a high amount of oxygen. This excludes fresh organisms but
209 indicates again (highly) mature OM. Minerals on the surface of filamentous kerite (Fig. 1a-d),
210 of bulbous kerite (Fig. 1e), and of the spherical object, interpreted by Head et al. (2023) as a
211 pollen, are mostly Al-silicates, some with K, Na, and Ca. The flaky shape of the minerals
212 indicates clay minerals, one needle-shaped crystal is a Ti-oxide, possibly rutile.



213
214 **Figure 1.** EDS spectra obtained with the SEM of filamentous (a, b, c, d) and bulbous (e) kerite
215 objects. (a) Needle-shaped small object with high Ti-O contents (arrow; interpreted as rutile)
216 next to Al-silicates with minor amounts of Na, K, and Ca. (b) Spectrum of clear surface (arrow)
217 of kerite, showing only the kerite composition of C-N-O. (c) Spectrum of platy mineral grains
218 (arrow) with Al-Si and small contents of K and Fe, interpreted as a clay mineral. (e) Base
219 (arrow) of bulbous kerite, with high amounts of Al-Si. Samples are iridium-coated.

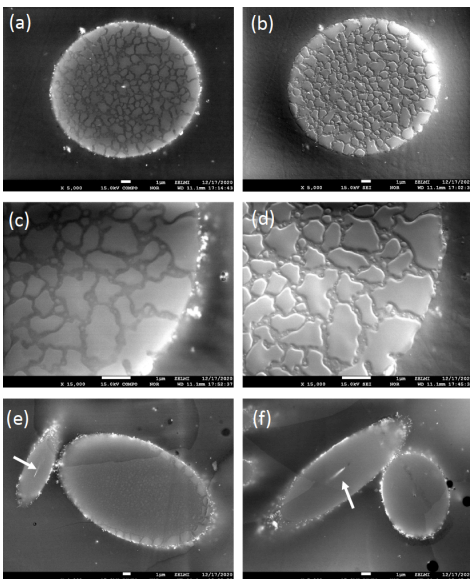


220
 221 **Figure 2.** EDS spectra of a spherical object (a) and a filamentous object (b). The spherical object
 222 shows Al-Si-K peaks, which can be interpreted as illite, whereas the filamentous object shows
 223 only the typical composition of kerite with C-N-O; both samples are iridium-coated.
 224



225

226 **Figure 3.** EDS data of flaky kerite, observed on sample V2008, a beryl crystal. (a, b, c, d) show
 227 the structure of kerite, in (a) with combined BSE detector for element contrast. The dark
 228 contrast compared to background beryl and other minerals indicates low average atomic
 229 number. (e) is the corresponding EDS spectrum with clear indication for Si, Al, Na, K, and Cl,
 230 next to C-N-O of kerite. (f) is EDS spectrum of beryl; note the low C-peak caused by carbon
 231 coating, compared to the large C-peak of kerite.
 232



233 **Figure 4.** BSE (a, c, d, e) and SE (b, d) of cross sections of filamentous kerite, embedded in
 234 epoxy. Note the discontinuous rim of high contrast indicating mineralized parts, and within
 235 the channel (e, f) also with high contrast (arrows). The mosaic pattern with different contrast
 236 in BSE (a, c) is seen in SE images (b, d) as slightly lower areas of approximately 200 nm width.
 237
 238

239 The EDS spectrum of the object, interpreted as pollen by Head et al. (2023), also shows
 240 the presence of Al and Si, together with the typical C-N-O peaks (Fig. 2). The EDS spectrum of
 241 the object, interpreted by Head et al. (2023) as trichome 'museum dust' (Fig. 3) shows no Al-
 242 Si, but the C-N-O ratios are very similar to those of the mineralized filaments, and therefore
 243 we have no doubts that this is also fossilized OM.
 244

245 3.4 EMPA data

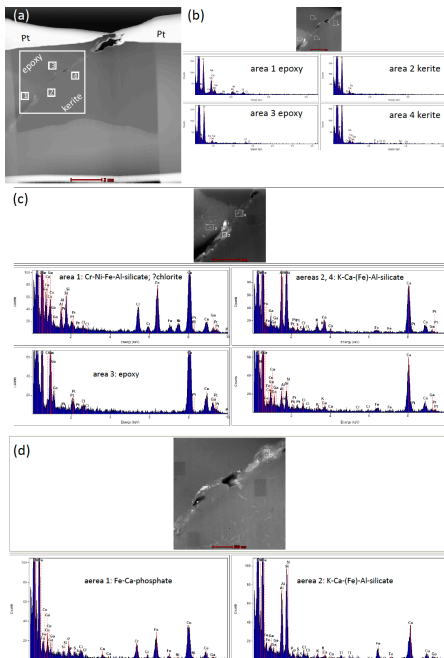
246 In BSE images of cross sections of filamentous kerite we see a discontinuous mineralized rim
 247 (Fig. 4). In combination with the element mappings (see images in figures 8 to 11 in Franz et
 248 al. 2022, and figures S6, S7 in the supplement to Franz et al. 2022), we can safely conclude
 249 that the mineralized rim consists dominantly of Al-silicates. Some other minerals such as Ca-
 250 phosphate or silica occur only in isolated spots and do not cover the whole rim. Over a distance
 251 of approximately 1 μm the filament shows a higher contrast rim in BSE images, indicating a
 252 higher average atomic number, consistent with our interpretation that this is caused by a
 253 mineralized, impregnated rim of dominantly Al-silicates. In the internal structure of the
 254 filament, a mosaic pattern can be observed with approximately 200 nm wide channels, also

255 indicated by different element contrast (Fig. 4a, b). In SE images (Fig. 4c, d) a slightly lower
256 position of the channels is seen, caused by different behavior during polishing. This internal
257 structure is compatible with fossilized material, not with fresh cells of trichomes.

258 3.5 TEM data

259 In addition to the TEM investigations we presented in Franz et al. (2017), we cut a new focused
260 ion beam (FIB) foil from a filamentous object (Fig. 5). The foil covers the embedding material
261 epoxy (characterized by typical Cl-content), the approximately 500 nm wide rim and kerite
262 (with dominantly C-O and N). The rim consists of a mixture of different minerals, which can be
263 distinguished by different contrast in the HAADF images. EDAX spectra indicate dominantly
264 Al-silicates with minor amounts of K, Ca, and Fe, and Fe-Ca-phosphate. This is different from
265 the type of biomineralization in trichomes, shown by Mustafa et al. (2017, 2018) and Ensikat
266 et al. (2017).

268



269 **Figure 5.** Analytical EDAX-TEM results on a FIB from the rim of a filamentous kerite object.
270 Note for all spectra that Ga-peaks are due to the Ga ion cutting, Cu peaks originate from the
271 copper grid, and Pt from the platinum holder. (a) Overview of the FIB foil; white frame
272 indicates position of (b) high-angular annular dark-field (HAADF) image and EDAX spectra of
273 kerite and embedding material epoxy. (c) Detail of (b) with EDAX spectra of three inclusions,
274 interpreted as possibly chlorite and a complex Al-silicate, possibly a clay mineral. (d) Detail of
275 (b) with EDAX spectra of two inclusions, a Fe-Ca-phosphate and a complex Al-silicate.

277

278 3.6 IR spectra

279 Head et al. (2023) criticize our IR spectra and argue that we should have used modern fungal
280 chitin standards for comparison and a more detailed comparison with sub-fossil and fossil
281 fungi. Since we knew that the Volyn biota experienced temperatures near 300 °C, comparison

hat gelöscht: transmission electron microscope (

hat gelöscht:)

hat gelöscht: a

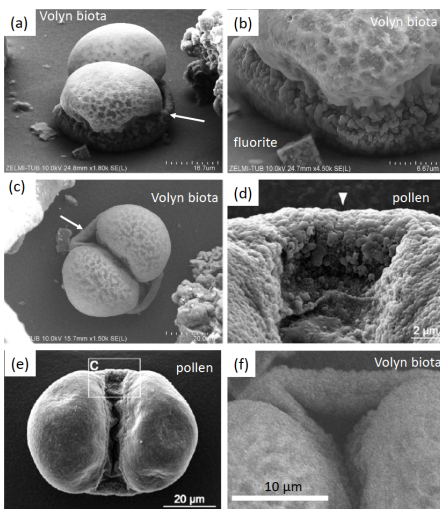
285 with modern fungi did not seem appropriate to us. Instead, we followed the procedure by
286 Loron et al. (2019) and the thermal degradation studies of chitosan (Wanjun et al., 2005;
287 Zawadzki and Kaczmarek, 2010; Vasilev et al., 2019). These are clearly consistent with our
288 conclusion that chitosan is a constituent of the kerite material.

289

290 4 Comparison of kerite morphology

291 Head et al. (2023) present evidence for strong similarity of one object of our sample collection
292 with pollen of an extinct conifer. The similarity is indeed striking, but we want to stress
293 important differences (Fig. 6):

294



295

296 **Figure 6.** SEM images for direct comparison of kerite object from Volyn biota (a, b, c, f) and
297 *Pinus* pollen (d, e) from Head et al. (2023). Note that the kerite object is sitting firmly on base
298 consisting of OM (a, b), whereas pollen are free objects. The surface of kerite is characterized
299 by dents (b), whereas the pollen shows a microrogulate surface (d). What is described from
300 pollen as air sacs (d, e) sits on a similar height as the pollen grain itself (d), whereas what we
301 described as a sheath comes from the base of the kerite object (arrows in a and c). This sheath
302 shows some inward folding (f), which is not seen in the air sac of the pollen.

303

304 The kerite object is sitting firmly on a base consisting of OM (Fig. 6a, b), whereas pollen
305 are free objects. The surface of kerite is characterized by dents (Fig. b), whereas the pollen
306 shows a microrogulate surface (Fig. d). What is described from pollen as air sacs (Fig. 6d, e)
307 sits on a similar height as the pollen grain itself, whereas what we described as a sheath
308 comes from the base of the kerite object (arrows in Fig. 6a, c). This sheath shows some inward folding
309 (Fig. 6f), which is not seen in the air sac of the pollen.

310 The other object, which Head et al. (2023) interpret as a plant hair (figure 3 j, k, l; in Franz
311 et al. 2023a) due to the similarity to ‘museum dust’, also sits firmly on a base. If such a delicate
312 object like unfossilized trichomes was transported down into the chamber (where it was
313 sampled), it is difficult to imagine that it survived the transport.

314 Head et al. (2023) restrict their criticism to these two objects but do not mention the fact
315 that the large majority of objects we presented has a different morphology, with filaments up
316 to the mm-size, bulbous objects, objects with irregular shape etc. None of these objects is

317 similar to trichomes. Also, they do not mention the internal structure with a channel, which
318 we documented in detail (figure 11 in Franz et al., 2023a), and which is obvious also in BSE
319 images (Fig. 4). They also do not mention the presence of Bi(Te,S) biomineralization, which we
320 documented (figure 10 in Franz et al., 2023). To the best of our knowledge, this type of
321 biomineralization was not observed in trichomes.

322

323 5 Age of the fossils

324 Popov (2023) questioned the minimum age of the organic matter, which we proposed as 1.5
325 Ga, based on the Ar-Ar laser ablation data (Franz et al., 2022a) of muscovite in a pseudomorph
326 after beryl. He proposed a sequence of events, starting with the intrusion of the granites and
327 the pegmatites at approximately 1.76 Ga (Shumlyanskyy et al., 2017, 2021), cooling and
328 pseudomorph formation due to a hydrothermal event at 1.5 Ga, then again cooling,
329 introduction of organic matter, then a second hydrothermal event, which converted
330 muscovite into tobelite and K-feldspar into buddingtonite. The age of the second event could
331 have been early Phanerozoic, based on our data (Franz et al., 2022b) of dating attempts of the
332 kerite itself, which produced in Popov's (2023) wording an isochrone of 493 ± 98 (1s) Ma, but
333 which we considered only as a reference line due to the large uncertainty. In this sequence of
334 events the breccia formation is missing, but this event is important: It fractionated feldspar
335 and quartz into cm-sized, irregular pieces, including a large piece of pegmatitic beryl. This
336 event must have occurred before the pseudomorph formation, because the delicate
337 pseudomorph, consisting of a rather loose framework of muscovite and bertrandite would not
338 have survived the brecciation. But the breccia is cemented by black opal (pigmented by
339 hydrocarbons), and OM must have been present before precipitation of opal. Therefore, the
340 sequence of events after the intrusion must have been: Presence of organic matter,
341 brecciation, pseudomorph formation at 1.5 Ga in one event, first with muscovite formation,
342 then during decay of the kerite and production of NH_4^+ tobelite and buddingtonite (including
343 formation of secondary, C-H bearing fluid inclusions in low-T beryl), then further cooling. It
344 was made clear in our text that "...the fluid composition changed during the pseudomorph
345 formation, starting with F-dominated K-rich fluids producing pure F-muscovite, followed by
346 alternating NH_4 -rich and K-rich compositions, producing oscillatory growth zones in
347 buddingtonite (Fig. 5e) and ending with a late K-rich fluid (producing some outer K-rich zones
348 in buddingtonite; Fig. 5d)." This is the same conclusion as in our first analysis of the
349 pseudomorph's texture (Franz et al., 2017) and clear from the summary figure 13, illustrating
350 the sequence of processes in one single geological event. We feel misinterpreted by Popov
351 (2023), who wrote that in our second study we had changed our mind.

352 There might have been additional hydrothermal events since 1.5 Ga, caused e. g. by the
353 Neoproterozoic Volyn Large Igneous Province at approximately 600 Ma or later Devonian
354 rifting of the Prypyat aulacogen (Shumlyanskyy et al., 2016), but none of these events is
355 documented up to now in the pegmatites of the Volyn field. We fully agree with Popov (2023)
356 that the late-stage development of pegmatites including later overprinting by hydrothermal
357 events may point to a protracted history. However, for the Volyn locality, the late-stage
358 development is documented in Lazarenko et al. (1973) and in a study of dissolution of Volyn
359 beryl crystals with the formation of typical and diagnostic etching (Franz et al., 2023b).

360

361 6 Origin of kerite - biotic or abiotic

362 Head et al. (2023) conclude their discussion with "We have doubts whether any of the in-situ
363 Volyn 'biota' is organic in origin", based on references to the low $\delta^{13}\text{C}$ values obtained via
364 experiments with Fischer-Tropsch-type synthesis (FTT) under hydrothermal conditions in the

hat gelöscht: BSE

hat gelöscht: e, f

367 presence of metallic Fe. From a starting composition with an assumed value for $\delta^{13}\text{C}$ of -20 ‰,
368 different organic compounds were obtained with a rather uniform composition of -50 ‰
369 (McCullum and Seewald, 2006). Abiotic synthesis of nitrogen-bearing organic carbon species,
370 such as amino acids, is thermodynamically favored by molecular H_2 , which is produced by
371 serpentinization of Fe-rich mantle-derived rocks (Ménez et al., 2018). The presence of Fe-rich
372 minerals as catalyst for the production of abiotic carbonaceous material in serpentinites (Nan
373 et al., 2021) is not a good analogue for the granitic environment, in which Fe-rich minerals are
374 generally scarce. An FTT process is unlikely in the current geological setting of an Fe-poor
375 granite-pegmatite system.

hat verschoben (Einfügung) [1]

376 Source of carbon for abiotic synthesis in Volyn should be the mantle with a uniform $\delta^{13}\text{C}$
377 value of -5 ‰ (Marty et al., 2013, and references therein), because the Korosten pluton is
378 comprised mainly of mantle-derived granitic, gabbroic, and anorthositic rocks (Shumlyansky
379 et al., 2017, 2021). Assuming a similar fractionation of -30 ‰ for a source with $\delta^{13}\text{C}$ of -5 ‰,
380 a composition of abiotic kerite should have values of -35 ‰, but many kerite bulk samples
381 have much lower values between -40‰ and -48‰. According to the model of abiotic origin,
382 mantle-derived fluids should also be the source for nitrogen. The N-isotopic signature of the
383 mantle scatters from -25 ‰ to +15, with most values around -5 ± 3 ‰ Cartigny (2005),
384 therefore a mantle source is less likely for the Volyn locale, with positive $\delta^{15}\text{N}$ values up to 10
385 ‰ throughout. A more detailed description of isotopic composition of the kerite organic
386 matter might be possible by in-situ methods. Such methods are currently not available for us,
387 but we will explore the possibility for cooperation with other laboratories.

hat gelöscht: ↵

388 An alternative source might be the country rocks of the Korosten pluton, but this would
389 require large amounts of C- and N-rich fluids, and there is no geological evidence for such
390 fluid-rock interactions. They should have left their signature also within the granites, which
391 are the hosts of the pegmatites. Yushkin (1996) presented analyses of different proteins in
392 kerite and used it as an argument that abiotic synthesis is possible. However, he starts from
393 the assumption of abiotic origin and did not consider the possibility of fossil material. The
394 large amounts of kerite of several kg recovered from the mine (Ginzburg et al., 1987) is in our
395 view more consistent with biomass accumulation; what has been described as abiotic
396 formation of carbonaceous material was observed in small amounts in thin section only (e. g.
397 Nan et al., 2021; Ménez et al., 2018).

hat gelöscht: a

hat nach oben verschoben [1]: The presence of Fe-rich minerals as catalyst for the production of abiotic carbonaceous material in serpentinites (Nan et al., 2021) is not a good analogue for the granitic environment, in which Fe-rich minerals are generally scarce. Yush

399 Summary and open questions

400 Although the morphology of two objects, selected by Head et al. (2023) show a striking
401 similarity to recent organisms, the combination of all observations is much more in favor of
402 fossil organisms: The occurrence in the mine as part of the deep biosphere; a large variety of
403 morphologically different objects, which however have all the same type of rim
404 mineralization; their brittle behavior; the internal structure with a channel in the filaments;
405 the presence of biomineral inclusions of Bi(Te,S).

406 Further studies on the molecular composition, i. e. certain biomarkers, will help to
407 characterize kerite in more detail and give information about the type of organisms, which
408 requires, however, more material. This is under the current situation in Ukraine not available.

Formatiert: Einzug: Erste Zeile: 0.75 cm

409 We are aware that our single age determination of 1.5 Ga for the hydrothermal
410 overprinting of the pegmatites should be verified or falsified by ages on different minerals
411 and/or different isotope systems. If more and better data will be available, we are happy to
412 change the interpretation, but with the current available data the presented interpretation

420 seems to be the best one. We are currently working on Rb-Sr data with the laser-ablation
421 system from the same sample, which was determined by Ar-Ar and which can be applied to
422 both minerals, muscovite and feldspar. Additional sample material with white mica and
423 feldspar is also available and will be studied.

424 Fluid inclusion studies might further help to clarify the origin of kerite (Vozniak et al.,
425 2012, and references therein; Kalyuzhnyi et al., 1971). Liu et al. (2022) observed whewellite
426 (CaC₂O₄·H₂O) in CO₂-N₂-CH₄-vapor of fluid inclusions in topaz, thought as a product of
427 oxidation of organic material with an alkaline fluid. In-situ determination of C- and N-isotopes,
428 and possibly also other stable isotopes (e.g. O, S) might also help to further clarify the type of
429 organisms, their internal structure, and their origin.

431 *Data availability.* All data are as figures in the text or in the cited references.

432 *Supplement.* There is no supplement to this article.

433 Author contributions. GF concept, figures, and writing; VK writing, FTIR; VC and PL information
434 about the sampling and occurrence.

435 *Competing interests.* The authors declared that they have no competing interests.

436 *Acknowledgements.* We thank Anja Schreiber and Richard Wirth for permission to use
437 unpublished TEM data.

438 *Financial support.* VK acknowledges funding by Alexander von Humboldt foundation.

439 References

440 Barton, M. D., and Young, S.: Non-pegmatitic deposits of beryllium: Mineralogy, geology,
441 phase equilibria and origin. *Rev. Mineral. Geochem.*, 50, 591-691, 2002.

442 Cartigny, P., Stable isotopes and the origin of diamond, *Elements*, 1, 79-84, 2005.

443 Ciarniello, M., Moroz, L. V., Poch, O., Vinogradoff, V., Beck, P., Rousseau, B., Jstiqomah, I.,
444 Sultana, R., Raponi, A., Schroeder, S., Kappel, D., Quirico, E., Filacchione, G., Pommerol, A.,
445 Mennella, V., and Pilorget, C.: VIS-IR spectroscopy of mixtures of ice, organic matter and
446 opaque minerals in support of minor bodies remote sensing observations, EPSC Abstracts 13,
447 1467-1468, 2019.

448 Durand, B.: Sedimentary organic matter and kerogen. Definition and qualitative importance
449 of kerogen, in Kerogen—Insoluble Organic Matter from Sedimentary Rocks (B. Durand, Ed.),
450 pp. 13–34, Editions Technip, Paris, 1980.

451 Ensikat, H.-J., Mustafa, A., and Weigend, M.: Complex patterns of multiple biomineralization
452 in single-celled plant trichomes of the Loasaceae, *Amer. J. Botany*, 104, 195-206, 2017.

453 Franz, G. Khomenko, V. Vishnyevskyy, A. Wirth, R. Nissen, and J. Rocholl, A.: Biologically
454 mediated crystallization of buddingtonite in the Paleoproterozoic: Organic-igneous
455 interactions from the Volyn pegmatite, Ukraine, *Amer. Mineral.* 102, 2119-2135, 2017.

456 Franz, G., Sudo, M., and Khomenko, V.: ⁴⁰Ar/³⁹Ar dating of a hydrothermal pegmatitic
457 buddingtonite-muscovite assemblage from Volyn, Ukraine, *Eur. J. Mineral.*, 34, 7-18.
458 doi.org/10.5194/ejm-34-7-2022, 2022a.

hat gelöscht: iews

hat gelöscht: in

hat gelöscht: ogy

hat gelöscht: and

hat gelöscht: istry

hat formatiert: Schriftart: (Standard) +Textkörper (Calibri),
Englisch (USA)

hat formatiert: Schriftart: (Standard) +Textkörper (Calibri),
Englisch (USA)

hat formatiert: Schriftart: (Standard) +Textkörper (Calibri),
Englisch (USA)

hat formatiert: Schriftart: (Standard) +Textkörper (Calibri),
Englisch (USA)

hat formatiert: Schriftart: (Standard) +Textkörper (Calibri),
Englisch (USA)

hat formatiert: Schriftart: (Standard) +Textkörper (Calibri),
Englisch (USA)

hat formatiert: Schriftart: (Standard) +Textkörper (Calibri),
Englisch (USA)

hat formatiert: Schriftart: (Standard) +Textkörper (Calibri),
Englisch (USA)

hat formatiert: Schriftart: (Standard) +Textkörper (Calibri),
Englisch (USA)

hat formatiert: Schriftart: (Standard) +Textkörper (Calibri),
Englisch (USA)

hat formatiert: Schriftart: (Standard) +Textkörper (Calibri),
Englisch (USA)

hat formatiert: Schriftart: (Standard) +Textkörper (Calibri),
Englisch (USA)

hat formatiert: Schriftart: (Standard) +Textkörper (Calibri),
Englisch (USA)

hat formatiert: Schriftart: (Standard) +Textkörper (Calibri),
Englisch (USA)

hat formatiert: Schriftart: (Standard) +Textkörper (Calibri),
Englisch (USA)

hat formatiert ... [1]

hat formatiert ... [2]

hat formatiert ... [3]

hat formatiert ... [4]

hat formatiert ... [5]

hat formatiert ... [6]

hat formatiert ... [7]

hat formatiert ... [9]

Formatiert ... [8]

hat formatiert ... [10]

hat formatiert ... [11]

hat formatiert ... [12]

hat formatiert: Englisch (USA)

hat formatiert: Schriftart:

hat gelöscht: ,

hat gelöscht: .

hat gelöscht: .

hat formatiert: Englisch (USA)

475 Franz, G., Lyckberg, P., Khomenko, V., Chornousenko, V., Schulz, H.-M., Mahlstedt, N., Wirth,
476 R., Glodny, J., Gernert, U., and Nissen, J.: Fossilization of Precambrian organic matter (kerite)
477 from the Volyn pegmatite, Ukraine. *BioGeosciences*, 19, 1795-1811, 2022b.

478 Franz, G., Khomenko, V., Lyckberg, P., Chornousenko, V., Struck, U., Wirth, R., Gernert, U., and
479 Nissen, J.: The Volyn biota (Ukraine) – indications for 1.5 Gyr old eucaryotes in 3D-
480 preservation, a spotlight on the ‘boring billion’. *BioGeosciences*, 20, 1901-1924,
481 doi.org/10.5194/bg-20-1901-2023, 2023a.

482 Franz, G., Vyschnevskiy, O. A., Khomenko, V. M., Lyckberg, P., and Gernert, U.: Etch pits in
483 heliodor and green beryl from the Volyn pegmatites, Northwest Ukraine: A diagnostic feature,
484 *Gems & Gemology*, 59(3) 324-339, doi.org/10.5741/GEM;S.59.3.324, 2023b.

485 Ginzburg, A.I., Bulgakov, V.S., Vasilishin, I.S., Luk'yanova, V.T., Solntseva, L.S., Urmenova, A.M.,
486 and Uspenskaya, V.A.: Kerite from pegmatites of Volyn, *Dokl. Akad. Nauk SSSR*, 292, 188–191,
487 1987 (in Russian).

488 Gorlenko, V.M., Zhmur, S.I., Duda, V.I., Osipov, G.A., Suzina, N.E., and Dmitriev, V. V.: Fine
489 structure of fossilized bacteria in Volyn kerite, *Orig. Life Evol. Biosph.*, 30, 567–577, 2000.

490 Head, M. J., Riding, J. B., O'Keefe, J. M. K., Jeiter, J., and Gravendyck, J.: Comment on Franz et
491 al. 2023: A reinterpretation of the 1.5 billion year old Volyn ‘biota’ of Ukraine, and discussion
492 on the evolution of eucaryotes, *BioGeosciences*,
493 <https://egusphere.copernicus.org/preprints/2023/egusphere-2023-2748/>, 2023.

494 Kalyuzhnyi V. A., Voznyak, D. K., and Gigashvili, G. M.: Mineral-forming fluids and mineral
495 paragenesis of chamber pegmatites of Ukraine, Kyiv: Naukova Dumka, 216 pp., 1971 (in
496 Ukrainian).

497 Lazarenko, E. K., Pavlishin, V. J., Latysh, V. T., and Sorokon, Ju. G.: Mineralogy and genesis of
498 the chamber pegmatites from Volyn, (in Russian) Lvov, Vysskaja shkola, 360 pp, 1973.

499 Liu, Y., Schmidt, C., and Li, J.: Peralkalinity in peraluminous granitic pegmatites. I. Evidence
500 from whewellite and hydrogen carbonate in fluid inclusions, *Amer. Mineral*, 107, 233-238,
501 2022.

502 Loges, A., Manni, M., Louvel, M., Wilke, M., Jahn, S., Welter, E., Borchert, M., Qiao, S., Klemme,
503 S., and Keller, B. G.: Complexation of Zr and Hf in fluoride-rich hydrothermal aqueous fluids
504 and its significance for high field strength element fractionation, *Geochim. Cosmochim. Acta*,
505 366, 167-181, doi.org/10.1016/j.gca.2023.12.013, 2023.

506 Loron, C. C., François, C., Rainbird, R. H., Turner, E. C., Borensztajn, S., and Javaux, E. J.: Early
507 fungi from the Proterozoic era in Arctic Canada, *Nature* 570.7760: 232-235, 2019.

508 Lu'kyanova, V. T., Lobzova, R. V., and Popov, V. T.: Filiceous kerite in pegmatites of Volyn,
509 *Izvestiya Ross. Akademii Nauk Ser. Geologicheskaya*, 5, 102-118, 1992 (in Russian).

510 Mäder, U. K., Ramseyer, K., Daniels, E. J., and Althaus, E.: Gibbs free energy of buddingtonite
511 (NH₄AlSi₃O₈) extrapolated from experiments and comparison to natural occurrences and
512 polyedral estimation, *Eur. J. Mineral.*, 8, 755-766, 1996.

513 Marty, B., Alexander, O'D., and Raymond, S. N.: Primordial origins of Earth's carbon. *Reviews*
514 *Mineral. Geochem.*, 75, 149-181, 2013.

515 [McCollom, T. M., and Seewald, J. S.: Carbon isotope composition of organic compounds
516 produced by abiotic synthesis under hydrothermal conditions, *Earth Planet. Sci. Lett.*, 243,
517 74-84, doi.org/10.1016/j.epsl.2006.01.027, 2006.](#)

518 Ménez, B., Pisapia, C., Andreani, M., Jamme, F., Vanbellingen, Q., et al.: abiotic synthesis of
519 amino acids in the recesses of the oceanic lithosphere, *Nature*, 564 (7734), 59-63,
520 doi.org/10.1038/s41596-018-0684-z.hal-02111638, 2018.

521 [Moroz, L. V., Arnold, G., Korochantsev, A. V., and Wäsch, R.: Natural solid bitumens as possible
522 analogs for cometary and asteroid organics: 1. Reflectance spectroscopy of pure bitumens,](#)

hat gelöscht: o

hat gelöscht: N

hat formatiert: Englisch (USA)

hat formatiert: Englisch (USA)

hat gelöscht: .

hat gelöscht: e

hat gelöscht: ,

hat gelöscht: .

hat gelöscht: :

hat gelöscht: ,

Feldfunktion geändert

hat gelöscht: ,

hat gelöscht: ,

hat gelöscht: .

hat gelöscht: .

hat gelöscht: ¶

Nan, J., King, H. E., Delen, G., Meirer, F., Weckhysen, B. M., Guo, Z., Peng, X., and Plümer, O., The nanogeochemistry of abiotic carbonaceous matter in serpentinites from the Yap Trench, western Pacific Ocean, *Geology*, 49, 330-334, doi.org/10.1130/G48153.1, 2021. ¶

hat gelöscht: .

hat gelöscht: ,

hat gelöscht: et al.,

hat gelöscht: McCollom, T. M., and Seewald, J. S.: Carbon isotope composition of organic compounds produced by abiotic synthesis under hydrothermal conditions, *Earth Planet. Sci. Lett.* 243, 74-84, doi.org/10.1016/j.epsl.2006.01.027, 2006. ¶

548 [ICARUS, 134: 253-268, 1998.](#)
549 Mustafa, A., Ensikat, H.-J., and Weigend, M.: Ontogeny and the process of biomineralization
550 in the trichomes of Laosaceae, *Amer. J. Botany*, 104(3), 367-378, 2017.
551 Mustafa, A., Ensikat, H.-J., and Weigend, M.: Mineralized trichomes in Boraginales: complex
552 microscale heterogeneity and simple phylogenetic patterns, *Ann. Botany*, 121, 741-751, doi:
553 10.1093/aob/mcx191, 2018.
554 Nan, J., King, H. E., Delen, G., Meirer, F., Weckhuysen, B. M. Guo, Z., Peng, Z., and Plümper,
555 O.: The nanogeochemistry of abiotic carbonaceous matter in serpentinites from the Yap
556 Trench, western Pacific Ocean, *Geology*, 49, 330-334, doi.org/10.1130/G48153.1, 2021.
557 Popov, D. V.: Do pegmatites crystallise fast? A perspective from petrologically-constrained
558 isotopic dating, *Geosciences*, 13, 297, doi.org/10.3390/geosciences13100297, 2023.
559 Proshko, V. Ya., Bagmut, N. N., Vasilishin, I. S., and Panchenko, V. I.: Ammonium feldspars from
560 Volyn pegmatites and their radiospectroscopic properties, *Mineral. J. (Ukraine)*, 9, 67-71, 1987
561 (in Russian).
562 Shumlyanskyy, L., Nosova, A., Billström, K., Söderlund, U., Andréasson, P.-G., and
563 Kuzmenkova, O.: The U–Pb zircon and baddeleyite ages of the Neoproterozoic Volyn Large
564 Igneous Province: implication for the age of the magmatism and the nature of a crustal
565 contaminant, *Gff-Upsala*, 138(1), 17-30, 2016.
566 Shumlyanskyy L., Hawkesworth C., Billström K., Bogdanova S., Mytrokhyn O., Romer R.,
567 Dhuime B., Claesson S., Ernst R., Whitehouse M., [and](#) Bilan O.: The origin of the
568 Palaeoproterozoic AMCG complexes in the Ukrainian Shield: new U-Pb ages and Hf isotopes
569 in zircon, *Precam. Res.*, 292, 216-239, 2017.
570 Shumlyanskyy, L., Franz, G., Glynn, S., Mytrokhyn, O., Voznyak, D., and Bilan O.:
571 Geochronology of granites of the western part of the Korosten AMCG complex (Ukrainian
572 Shield): implications for the emplacement history and origin of miarolitic pegmatites, *Eur. J.*
573 *Min.*, 33, 703-716, 2021.
574 Vasilev, A., Efimov, M., Bondarenko, G., Kozlov, V., Dzidziguri, E., and Karpacheva, G.: Thermal
575 behavior of chitosan as a carbon material precursor under IR radiation, *IOP Conf. Ser.: Mater.*
576 *Sci. Eng.*, 693, 2019. doi.org/10.1088/1757-899X/693/1/012002.
577 Voznyak, D.K., Khomenko, V.M., Franz, G., and Wiedenbeck, M.: Physico-chemical conditions
578 of the late stage of Volyn pegmatite evolution: Fluid inclusions in beryl studied by
579 thermobarometry and IR-spectroscopy methods, *Mineral. J. (Ukraine)*, 34, 26–38, 2012 (in
580 Ukrainian).
581 Wanjun T., Cunxin W., [and](#) Donghua, C.: Kinetic studies on the pyrolysis of chitin and chitosan,
582 *Polym. Degrad. Stabil.*, 87, 389–394, 2005.
583 Yushkin, N. P.: Natural polymer crystals of hydrocarbons as models of prebiological organisms,
584 *J. Crystal Growth*, no. 167, 237-247, 1996.
585 Zawadzki, J., and Kaczmarek, H.: Thermal treatment of chitosan in various conditions,
586 *Carbohydr. Polym.*, 80, 394-400, 2010.
587 Zhmur, S. I.: Origin of Cambrian fibrous kerites of the Volyn region, *Lithol. Mineral Resour.*, 38,
588 55-73, 2003.

hat gelöscht: ,

hat formatiert: Englisch (USA)

hat gelöscht: brian

hat gelöscht: earch

Seite 12: [1] hat formatiert 015126540301 30.07.24 10:34:00

Schriftart: (Standard) +Textkörper (Calibri), Englisch (USA)

Seite 12: [2] hat formatiert 015126540301 30.07.24 10:34:00

Schriftart: (Standard) +Textkörper (Calibri), Englisch (USA)

Seite 12: [3] hat formatiert 015126540301 30.07.24 10:34:00

Schriftart: (Standard) +Textkörper (Calibri), Englisch (USA)

Seite 12: [4] hat formatiert 015126540301 30.07.24 10:34:00

Schriftart: (Standard) +Textkörper (Calibri), Englisch (USA)

Seite 12: [5] hat formatiert 015126540301 30.07.24 10:34:00

Schriftart: (Standard) +Textkörper (Calibri), Englisch (USA)

Seite 12: [6] hat formatiert 015126540301 30.07.24 10:36:00

Schriftart: (Standard) +Textkörper (Calibri), Englisch (USA)

Seite 12: [7] hat formatiert 015126540301 30.07.24 10:39:00

Schriftart: (Standard) +Textkörper (Calibri), 12 Pt., Nicht Kursiv, Englisch (USA)

Seite 12: [8] Formatiert 015126540301 30.07.24 10:41:00

Links, Leerraum zwischen asiatischem und westlichem Text nicht anpassen, Leerraum zwischen asiatischem Text und Zahlen nicht anpassen

Seite 12: [9] hat formatiert 015126540301 30.07.24 10:39:00

Schriftart: (Standard) +Textkörper (Calibri), 12 Pt., Nicht Kursiv, Englisch (USA)

Seite 12: [10] hat formatiert 015126540301 30.07.24 10:39:00

Schriftart: (Standard) +Textkörper (Calibri), 12 Pt., Nicht Kursiv, Englisch (USA)

Seite 12: [11] hat formatiert 015126540301 30.07.24 10:39:00

Schriftart: (Standard) +Textkörper (Calibri), 12 Pt., Nicht Kursiv, Englisch (USA)

Seite 12: [12] hat formatiert 015126540301 30.07.24 10:39:00

Schriftart: (Standard) +Textkörper (Calibri), 12 Pt., Nicht Kursiv, Englisch (USA)